This article is published as part of the *Dalton Transactions* themed issue entitled:

Molecular Magnets

Guest Editor Euan Brechin
University of Edinburgh, UK

Published in issue 20, 2010 of *Dalton Transactions*

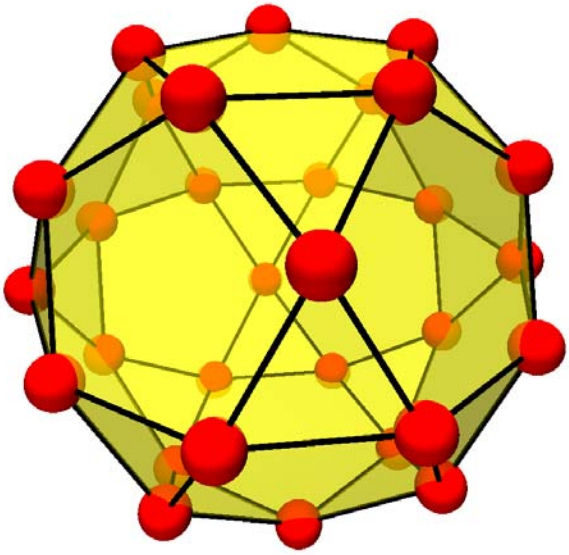

Image reproduced with permission of Jürgen Schnack

Articles in the issue include:

PERSPECTIVES:

COMMUNICATIONS:

Visit the *Dalton Transactions* website for more cutting-edge inorganic and organometallic research
www.rsc.org/dalton

Synthesis, crystal structure and magnetic properties of two oxalato-bridged dimetallic trinuclear complexes combined with a polar cation†

Emilio Pardo,[a] Cyrille Train,[a,b] Rodrigue Lescouëzec,[a] Kamal Boubekeur,[a] Eliseo Ruiz,[c] Francesc Lloret[d] and Michel Verdaguer*[a]

Received 8th February 2010, Accepted 7th April 2010
First published as an Advance Article on the web 26th April 2010
DOI: 10.1039/c002468f

Two isostructural heterometallic trinuclear oxalato-bridged complexes of formula $C_4[MCr_2(ox)_6(H_2O)_2]\cdot nH_2O$ (C^+ = 4-aminopyridinium; ox^{2-} = oxalate dianion; $M^{2+} = Mn^{2+}$, $n = 3$, **1**; $M^{2+} = Co^{2+}$, $n = 3.25$, **2**) have been synthesized by using direct self-assembly methods combining $C_3[Cr(ox)_3]$ and the chloride salts of the corresponding metal ion. The crystal structures of both compounds have been resolved by single-crystal X-ray diffraction. They crystallize in the $C2/c$ space group [$a = 11.5113(15)$ Å, $b = 20.250(3)$ Å, $c = 21.810(4)$ Å, $\beta = 100.447(10)°$, $V = 5161.6(3)$ Å^3, and $Z = 4$ for **1**, and $a = 11.4334(16)$ Å, $b = 20.243(2)$ Å, $c = 21.805(3)$ Å, $\beta = 101.113(9)°$, $V = 4951.9(11)$ Å^3, and $Z = 4$ for **2**]. The structures of **1** and **2** consist of discrete linear $[MCr_2(ox)_6]^{4-}$ bimetallic trinuclear units, pyridinium cations and crystallization water molecules. The linear trinuclear unit is built from a central *trans*-diaquametal(II), linked to two $Cr(ox)_3]^{3-}$ entities by oxalate bridges. One of the oxalate ions is coordinated to the central metal ion whereas the other two oxalate ligands are non-bridging. In the crystal, intermolecular hydrogen bonds involving oxalate ligands, water molecules and pyridinium cations, build a complex three-dimensional network. Variable-temperature magnetic susceptibility measurements for **1** and **2** indicate a weak ferromagnetic interaction ($J = +1.16$ and $+2.62/+2.70$ cm^{-1} for **1** and **2**, respectively) between the two terminal Cr^{III} ($S_{Cr} = 3/2$) and the central high-spin Mn^{II} ($S_{Mn} = 5/2$) and Co^{II} ($S_{Co} = 3/2$) ions. The nature and the amplitude of the exchange interaction are rationalized using DFT calculations and orbital interpretations.

Introduction

Coordination chemistry offers tools for the construction of a seemingly limitless range of supramolecular species based on metal–ligand coordinative interactions.[1] Among the wide variety of organic ligands employed to build polynuclear coordination compounds of first-row transition metal ions,[2] the oxalate bridge has shown special relevance in molecular magnetism because of its versatility to adopt many coordination modes[3–5] and to transmit magnetic exchange interaction.[6] With hexaaquametal ions it gives homometallic compounds where the exchange interaction is (strongly) antiferromagnetic, leading to singlet ground spin states.[7] Non-zero ground spin states[8] are obtained in heterometallic compounds when the metal ions have different number of unpaired electrons. Self-assembly using preformed complexes such as the $[Cr^{III}(ox)_3]^{3-}$ is efficient to reach heterometallic systems.[9–15] For example, when reacting the $[Cr^{III}(ox)_3]^{3-}$ building block with divalent hexaaqua-transition metal complexes, two and three dimensional (2D and 3D) heterometallic systems[16] are obtained. In many cases, this approach allows to control the architecture and therefore the physical properties of the final compound. Molecular chemists have successfully used this synthetic route to obtain multifunctional materials such as conducting ferromagnetic magnets or chiral magnets, the additional property being brought by the counter-ion and/or by the anionic oxalato-based network itself.[17] The counter ion plays a key role in the molecular assembly process. A better understanding of both the assembly process going on in solution and the host–guest interactions[17a] in the solid state should thus allow a fine control of the final compound topology and dimensionality. Lower dimension magnetic compounds may also be very interesting: on the one hand, they can be used as model compounds in order to better understand the magnetic interactions at play in 2D and 3D systems; on the other hand, they can exhibit slow relaxation of the magnetization,[18–20] which has recently received very high attention because of the molecular data storage possibilities offered by such systems.

As a first example of new compounds obtained with polar cations, we report here the synthesis, the crystal structure, the magnetic properties and their theoretical interpretation, of two new bimetallic trinuclear complexes,[21] $C_4[MnCr_2(ox)_6(H_2O)_2]\cdot 3H_2O$ (**1**) and $C_4[CoCr_2(ox)_6(H_2O)_2]\cdot 3.25H_2O$ (**2**) where C^+ is the 4-aminopyridinium polar cation (Scheme 1).

[a]*Institut Parisien de Chimie Moléculaire, Université Pierre et Marie Curie-Paris 6, UMR 7201, F-75252, Paris, France. E-mail: Michel.verdaguer@upmc.fr; Fax: 00 33 1 44 27 38 41; Tel: 00 33 1 44 27 30 59*
[b]*Laboratoire National des Champs Magnétiques Intenses, UPR CNRS 3228, 25 rue des Martyrs, B.P. 166, 38042, Grenoble cedex 9, France; Université Joseph Fourier, BP 53, F-38041 Grenoble Cedex 9, France*
[c]*Departament de Química Inorgànica and Institut de Recerca de Química Teòrica i Computacional, Universitat de Barcelona, Diagonal 647, E-08028, Spain*
[d]*Departament de Química Inorgànica, Instituto de Ciencia Molecular (ICMOL). Universitat de València, 46980, Paterna, València, Spain*

† Electronic supplementary information (ESI) available: Crystal packing of **1** and field dependence of M of **1** and **2**. CCDC reference numbers 762572 and 762573. For ESI and crystallographic data in CIF or other electronic format see DOI: 10.1039/c002468f

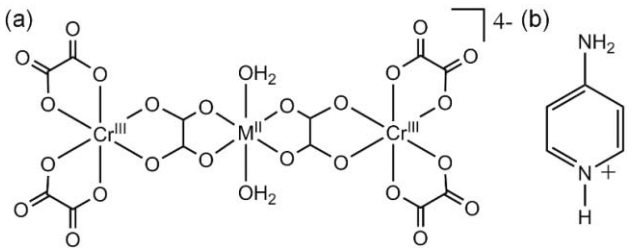

Scheme 1 Structural formulae of the (a) linear oxalato-bridged dimetallic trinuclear unit and (b) 4-aminopyridinium cation.

Experimental

Materials

The $MnCl_2{\cdot}4H_2O$ and $CoCl_2$ salts, and 4-aminopyridine were purchased from commercial sources and used as received. $(NH_4)_3[Cr(ox)_3]{\cdot}3H_2O$ was prepared by following a previously reported method.[22] Elemental analyses (C, H, N) were carried out by the Microanalytical Service of the Université Pierre et Marie Curie.

Preparations

4-Aminopyridinium chloride (C^+,Cl^-). This compound was prepared from the commercial 4-aminopyridine. 9.41 g of 4-aminopyridine (100 mmol) were dissolved in 40 mL of hydrochloric acid 37%. The solution was allowed to evaporate in air. After several days, a white polycrystalline solid was collected by filtration, washed with THF and diethyl ether and dried under vacuum (12.64 g, 97%). Elemental analysis calculated (%) for $C_5H_7N_2Cl$ (130.5): C 45.98, H 5.36, N 21.46; found: C 46.29, H 4.98, N 21.52; ^{1}H NMR ([D_6]DMSO): 7.013 (d, 2H; 3-H and 5-H of $C_5H_4NH(NH_2)$), 8.244 (d, 2H; 2-H and 6-H of $C_5H_4NH(NH_2)$), 8.344 (s, 2H; NH_2), 13.805 (s, 1H; NH); IR (KBr): ν = 3344 and 3196 (N–H), 3047 (C–H), 1654 (–NH_2) cm^{-1}.

$C_3[Cr(ox)_3]{\cdot}2H_2O$. Complex $C_3[Cr(ox)_3]{\cdot}2H_2O$ was obtained from a metathesis from the previously isolated ammonium complex $(NH_4)_3[Cr(ox)_3]{\cdot}3H_2O$[22] (2.12 g, 5 mmol), with $AgNO_3$ (2.55 g, 15 mmol) and (C^+, Cl^-) (1.96 g, 15 mmol) in 10 mL of water and 5 mL of methanol. The solution was evaporated to dryness. The solid was washed with ethanol, acetone and diethyl ether and dried under vacuum (2.29 g, 72%). Analysis calculated for $C_{21}H_{25}CrN_6O_{14}$ (637) C 39.56, H 3.92, N, 13.19; found: C 40.12, H 3.77, N 13.08; IR (KBr) 3432 (OH), 3059, 3042 2961 and 2929 (CH), 1652 (NH_2), 1710 and 1686 (CO) cm^{-1}.

$C_4[MnCr_2(ox)_6(H_2O)_2]{\cdot}3H_2O$ (1). Complex **1** was obtained by reaction of $C_3[Cr(ox)_3]{\cdot}2H_2O$ (1 mmol, 0.637 g) with $MnCl_2{\cdot}4H_2O$ (0.5 mmol, 0.099 g) in 5 mL of water. Large dark brown hexagonal plate-like single crystals of **1** suitable for X-ray diffraction were grown by slow vapor diffusion of ethanol into the aqueous solutions of **1** at r.t. after several days (2.29 g, 72%). Elemental analysis calculated (%) for $C_{32}H_{38}Cr_2MnN_8O_{29}$ (1157.46): C 33.18, H 3.28, N 9.68; found: C 33.59, H 2.79, N 10.01; IR (KBr): ν = 3243 (N–H), 3045 and 3011 (C–H), 1708, 1687, 1650 cm^{-1} (C–O).

$C_4[CoCr_2(ox)_6(H_2O)_2]{\cdot}3.25H_2O$ (2). Complex **2** was synthesized in a similar manner to complex **1** by reaction of $C_3[Cr(ox)_3]{\cdot}2H_2O$ (1 mmol, 0.637 g) with $CoCl_2$ (0.5 mmol, 0.065 g) in 5 mL of water. Dark brown hexagonal plate-like single crystals of **2** suitable for X-ray diffraction were grown by slow vapor diffusion of ethanol into the aqueous solutions of **2** at r.t. after several days (2.29 g, 72%). Elemental analysis calculated (%) for $C_{32}H_{38.5}CoCr_2N_8O_{29.25}$ (1166.08): C 32.93, H 3.30, N 9.60; found: C 33.12, H 2.82, N 9.98; IR (KBr): ν = 3265 (N–H), 3041 and 3022 (C–H), 1706, 1684, 1648 cm^{-1} (C–O).

Physical techniques

IR spectra of complexes **1** and **2** (4000–400 cm^{-1}) were recorded with a Bruker IF S55 specrophotometer on samples prepared as KBr pellets. Variable temperature (2.0–300 K) magnetic susceptibility measurements were carried out with a SQUID susceptometer using applied magnetic fields of 10000 G (T > 50 K) and 50 G (T < 50 K).

X-Ray crystallographic data collection and structure refinement

X-Ray diffraction data on single crystals of **1** and **2** were collected on a Nonius Kappa CCD diffractometer. Crystal parameters and refinement results are summarised in Table 1. Data collection and data reduction were done with the COLLECT and EVALCCD programs.[23] Empirical absorption corrections were carried out using SADABS.[24] The structures were solved by direct methods and refined with full-matrix least-squares technique on F^2 using the SHELXS-97 and SHELXL-97 programs[25] within the WINGX interface.[26] All non-hydrogen atoms were refined anisotropically. All the hydrogen atoms from the organic cations or water molecules were found in Fourier-difference maps (except those on crystallisation water molecules in **2**) but simply introduced in structure factors calculations. The final geometrical calculations and the graphical manipulations were carried out with PARST97 and CRYSTALMAKER programs, respectively.[27] A summary of the crystallographic data for **1** and **2** are listed in Table 1. Main bond

Table 1 Summary of crystallographic data for **1** and **2**

Formula	$C_{32}H_{38}Cr_2MnN_8O_{29}$	$C_{32}H_{32}CoCr_2N_8O_{29.25}$
Formula weight/g mol^{-1}	1157.46	1159.58
Crystal system	Monoclinic	Monoclinic
Space group	$C2/c$	$C2/c$
a/Å	11.5113(15)	11.4334(16)
b/Å	20.250(3)	20.243(2)
c/Å	21.810(4)	21.805(3)
β/°	100.447(10)	101.113(9)
V/Å^3	4999.9(13)	4951.9(11)
Z	4	4
ρ_c/g cm^{-3}	1.538	1.555
F(000)	2363.6	2356
μ/mm^{-1}	0.774	0.861
T/K	250(2)	250(2)
Reflect. collcd.	29683	12147
Reflect. indep. (R_{int})	7281 (0.0260)	7010 (0.0391)
Reflect. obs. [$I > 2\sigma(I)$]	5577	4327
Data/restraints/parameters	7281/9/335	7010/0/336
$R_1{}^a$ [$I > 2\sigma(I)$] (all)	0.0429 (0.0519)	0.0583 (0.0866)
$wR_2{}^b$ [$I > 2\sigma(I)$] (all)	0.1266 (0.1366)	0.1101 (0.1395)
S^c	1.003	1.068

^{a} $R_1 = \sum(|F_o| - |F_c|)/\sum|F_o|$. ^{b} $wR_2 = [\sum w(F_o^2 - F_c^2)^2/\sum w(F_o^2)^2]^{1/2}$. ^{c} $S = [\sum w(|F_o| - |F_c|)^2/(N_o - N_p)]^{1/2}$.

Table 2 Selected bond distances (Å) and angles (°) for **1** and **2**[b]

	M = Mn (**1**)	M = Co (**2**)
M(1)–O(1)	2.2383(17)	2.161(3)
M(1)–O(2)	2.2168(18)	2.138(3)
M(1)–O(13)	2.1496(19)	2.046(3)
Cr(1)–O(3)	2.0039(17)	2.011(3)
Cr(1)–O(4)	2.0154(17)	2.023(3)
Cr(1)–O(5)	1.9861(18)	1.995(3)
Cr(1)–O(6)	1.9837(17)	1.986(3)
Cr(1)–O(9)	1.9813(17)	1.982(3)
Cr(1)–O(10)	1.9765(19)	1.972(3)
O(2)–M(1)–O(1)	76.70(6)	79.28(10)
O(2)–M(1)–O(1)[a]	103.30(6)	100.72(10)
O(13)–M(1)–O(1)	86.05(7)	87.14(11)
O(13)–M(1)–O(1)[a]	93.95(7)	92.86(11)
O(13)–M(1)–O(2)	94.68(7)	93.39(11)
O(13)–M(1)–O(2)[a]	85.32(7)	86.61(11)
O(1)–M(1)–O(1)[a]	180.00(12)	180.00(14)
O(2)–M(1)–O(2)[a]	180.00(11)	180.000(1)
O(13)–M(1)–O(13)[a]	180.00(12)	180.000(1)
O(3)–Cr(1)–O(4)	82.38(7)	82.10(10)
O(5)–Cr(1)–O(3)	172.60(8)	172.31(12)
O(5)–Cr(1)–O(4)	92.62(7)	93.04(11)
O(6)–Cr(1)–O(3)	92.28(7)	92.18(11)
O(6)–Cr(1)–O(4)	92.84(7)	93.08(11)
O(6)–Cr(1)–O(5)	82.48(7)	82.09(11)
O(9)–Cr(1)–O(3)	94.75(8)	94.84(12)
O(9)–Cr(1)–O(4)	93.11(7)	93.04(11)
O(9)–Cr(1)–O(5)	90.96(8)	91.36(12)
O(9)–Cr(1)–O(6)	171.33(7)	171.26(11)
O(10)–Cr(1)–O(3)	92.72(8)	92.80(12)
O(10)–Cr(1)–O(4)	173.59(7)	173.50(12)
O(10)–Cr(1)–O(5)	92.64(8)	92.44(12)
O(10)–Cr(1)–O(6)	91.48(8)	91.12(12)
O(10)–Cr(1)–O(9)	83.14(7)	83.34(11)

[a] Symmetry code = −1/2 −*x*, 1/2 − *y*, −*z*]. [b] Estimated standard deviations are given in parentheses.

lengths and angles for **1** and **2** are listed in Table 2. Crystallographic data (excluding structure factors) for the structures reported in this paper have been deposited at the Cambridge Crystallographic Data Centre as CCDC 762572 and CCDC 762573.†

Computational details

Electronic structure calculations based on density functional theory (DFT) were used to estimate exchange coupling constants that involves tiny energy differences.[28] A detailed description of the followed computational strategy can be found in previously published papers.[29] We focus our discussion here to its most relevant aspects. For a linear symmetric trinuclear complex assuming that there is no interaction between the external paramagnetic centers, the exchange contributions to the Hamiltonians (eqn (1) and (2)) allows the estimation of J values calculated from just two spin configurations described using a single determinant wavefunction. The high-spin solution with the same sign of the spin of the three atoms and a low spin configuration with the inversion of the spin of the central atom. Thus, in the case of the chromium(III)–manganese(II) complex taking into account an energy difference for each exchange interaction of $(2S_1S_2 + S_1)J$ with $S_1 < S_2$, the energy difference between both spin configurations is 18J while for the chromium(III)–cobalt(II) complex the energy difference is 12J.

In previous papers, we have analysed the effect of the basis set and the choice of the functional on the accuracy of the determination of the exchange coupling constants.[29c,30] Thus, we found that the hybrid B3LYP functional,[31] together with the basis sets proposed by Schaefer *et al.*, provide J values in excellent agreement with the experimental ones. We have employed an all electron basis set of triple-ζ quality proposed by Schaefer *et al.*[32] In the case of the chromium(III)–manganese(II) complex, we also tried a quadruple-ζ basis sets.[33] The calculations were performed with the Gaussian09 code[34] using guess functions generated with the Jaguar 7.0 code[35] introducing the ligand field effects,[36] in order to control the local charge and multiplicity of each atom.

The D values and the spin channel contributions for the complex **2** were calculated with the B3LYP functional[31] with the Orca code[37] using the same basis set than the Gaussian calculations. In such approach, the spin–orbit effects were introduced using a spin–orbit mean field method proposed by Neese[38] and recently modified to handle the hybrid functionals.[39]

Results and discussion

Our synthetic strategy to get first row transition metal(II)–chromium(III) oxalato-bridged complexes consists of the reaction of $C_3[Cr(ox)_3]$ with the transition metal chloride (Mn^{II} and Co^{II}). The metathesis insures the presence of only one type of cation in the reaction and allows the formation of high purity compounds in high yields. Crystals suitable for X-ray diffraction, were grown by slow vapour diffusion.

In the infrared spectra of **1** and **2**, the main absorptions occur in the region 1710–1640 cm^{-1} [1708, 1687, 1650 cm^{-1} (**1**) and 1706, 1684, 1648 cm^{-1} (**2**)] which correspond to the ν(C=O) stretching of the oxalate group. They show clearly two types of C=O, free (1708–1684 cm^{-1}) and coordinated (1650 cm^{-1}).

Description of the structures of $(C)_4[MnCr_2(ox)_6(H_2O)_2]\cdot 3H_2O$ (1) and $(C)_4[CoCr_2(ox)_6(H_2O)_2]\cdot 3.25H_2O$ (2)

The two compounds are isostructural. Their structures will be described together and compared when useful with the one of $TTF_4[MCr_2(ox)_6(H_2O)_2]$ (M^{II} = Mn and Co; TTF= tetrathiafulvalene).[21b,21c] Compounds **1** and **2** are comprised of discrete linear oxalato-bridged trinuclear [Cr_2M] entities [M = Mn (**1**) and Co (**2**)] (Fig. 1) bearing four negative charges. Four 4-aminopyridinium cations ensure the electroneutrality of the crystal. Within the [Cr_2M] unit, the central divalent metal ion M(II) sits on an inversion centre. It is linked to two equivalent tris(oxalato)chromate(III) moieties through a bridging

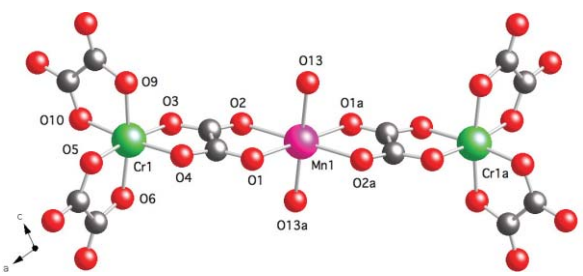

Fig. 1 Perspective view of the trinuclear anionic complex of $C_4[MnCr_2(ox)_6(H_2O)_2]\cdot 3H_2O$ (**1**) with the atom labelling for the coordination environment of the metals. Hydrogen atoms are omitted for clarity [symmetry code: (a) = −1/2 − *x*, 1/2 − *y*, −*z*].

bis-bidentate oxalate and to two water molecules in *trans* positions (Fig. 1). In the linear unit, the distances between metal atoms are Cr···Mn = 5.510(1) Å for **1** and Cr···Co = 5.429(1) Å for **2** and Cr(1)···Cr(1)^{a} = 11.019(2) Å for **1** and Cr(1)···Cr(1)^{a} = 10.859(2) Å, for **2**. These values are slightly higher than those in the corresponding $TTF_4[MCr_2(ox)_6(H_2O)_2]$.[21b,21c]

The two terminal Cr atoms in **1** and **2** show a slightly distorted octahedral environment which is formed by six oxygen atoms from three chelating oxalate groups in an approximate D_3 symmetry. The values of the chelate angles (α) are significantly smaller than those of an ideal octahedron ($\alpha = 90°$). The values of the metal–oxygen bond distances for the terminal oxalate ligands are slightly shorter than for the bridging ligands (see Table 2). They are however slightly longer than those of the tris(oxalato)chromate(III) potassium salt[40] and less dispersed than those of the TTF analogue.[21c]

The central M atom in **1** and **2** is surrounded by four oxygen atoms from two bridging oxalates of the two $[Cr(ox)_3]^{3-}$ units and two coordinated water molecules in a compressed octahedral environment. The compression is larger for the cobalt derivative than for the manganese one, as expected from the metal electronic structure, as in the TTF analogues.[21b,21c]

A packing diagram of the crystal of **1** is shown in Fig. 2. The trinuclear complexes build corrugated anionic sheets parallel to the *ac* plane. The layers are stacked in the *b* direction, well separated by cationic organic ones, together with water crystallization molecules. In the anionic layers, the water molecule $H_2O(13)$ coordinated to manganese(II) establishes hydrogen bonds to terminal oxalate oxygen atoms. The $O_{donor}\cdots O_{accept}$ distances are in the range 2.728(3)–2.891(3) Å for **1** and 2.725(5)–2.909(5) Å for **2**, respectively. These H-bonds shape the anionic layers in a pseudo-hexagonal 2D network, where six chromium(III) atoms surround a central manganese(II) atom (Fig. 2(a)). The chromium and the central metal are practically in the plane of the bridging oxalates. The Mn···Cr distances are 5.510(1) Å, 7.588(2) and 7.833(1) Å and the Cr···Cr distances are 6.634(1), 7.135(2) and 7.777(1) Å.

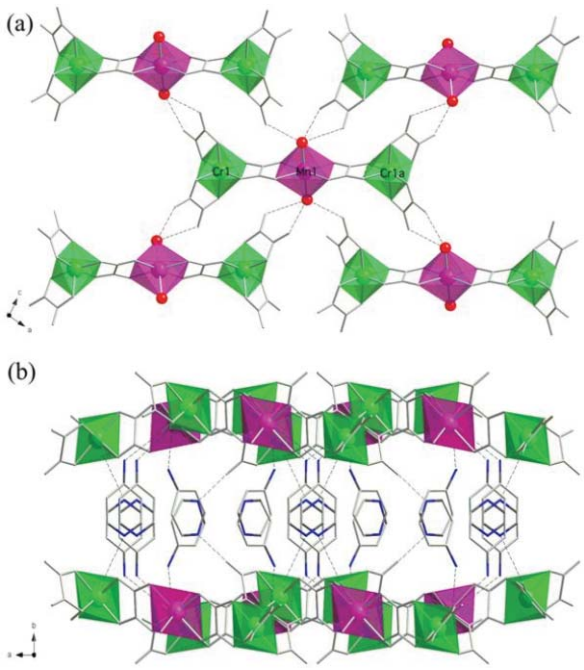

Fig. 2 Crystal packing of **1** along the *b* axis (a) and along *c* axis (b). In (a) dotted lines represent hydrogen bonds. Hydrogen atoms and crystallization water molecules have been omitted for clarity. The chromium and manganese surroundings are depicted as green and pink solid polyhedra.

The anionic layers and water molecules stack along the *b* direction. 4-Aminopyridinium cations are located between the layers and insure a good separation between them. The minimum distance between the same metal ions of different layers is 11.647(2) Å and 11.624(2) Å for **1** and **2**, respectively (Fig. S1(a), ESI†). In the cationic layers the mean direction of the longer axis of the molecules is orientated perpendicular to the oxalate layers. Both nitrogen atoms of the two kinds of 4-aminopyridinium cations build N–H···O bonds with terminal oxalate oxygen atoms. The N···O distances vary in the range 2.843(4)–3.164(5) Å and 2.877(8)–3.211(7) Å for **1** and **2**, respectively (Fig. S1(a), ESI†). These hydrogen bonds lead to the corrugated character of the anionic layers.

The cations are organised in columns. Starting from the two independent staggered cations, the twofold axis of the $C2/c$ space group leads to an assembly of four cations with a resulting net dipolar moment aligned along the *b* axis. Two of the cations are strictly parallel with strong π–π interactions, the centroid–centroid distance between the aromatic rings being 3.437(2) and 3.430(4) Å for **1** and **2**, respectively. Nevertheless, the centro symmetric character of the space group gives a head-to-tail arrangement of two adjacent groups of the four cations (Fig. S1(b), ESI†) and leads to a cancellation of the dipolar moment at the crystal level. No para- or ferro-electric properties can be observed. The crystallization water molecules participate in the H-bonding network either between them or with the oxalates in a complex manner due to the partial occupancy of sites O(15) and O(16) (1/3 in **1** and 1/2 in **2**). Short bond distance values indicate strong hydrogen bonds [O16···O15 = 2.679(17) Å (**1**) and 2.53(3) (**2**) and O16···O2 = 2.890(16) Å (**1**) and 2.92(2) Å) (**2**)]. $H_2O(14)$ is connected to terminal oxalate oxygen atoms belonging to two different trinuclear complexes. There is no H-bonding between water molecules and nitrogen atoms of the organic cations.

We conclude by comparing the structures of **1** and **2** with the one of $TTF_4[MnCr_2(ox)_6(H_2O)_2]$[21c] where all the TTF components are in the cationic form. All three compounds are built from four planar cationic organic molecules, 4-aminopyridinium and tetrathiafulvalenium, and the same trinuclear anionic unit Cr_2M bearing four charges in a 4 : 1 stoichiometry. They all present alternation of anionic layers of Cr_2M complexes separated by cationic organic layers. In both systems, the anionic layers are made of trinuclear Cr_2M complexes connected by hydrogen bonds from the water molecule coordinated to manganese(II). They build a pseudo-hexagonal lattice. In both systems, the four cationic molecules are coupled two by two, the TTF building a pseudo κ phase, whereas the 4-aminopyridinium cations are stacked in a wavy column. This difference is related to the fact that there are two crystallographically independent 4-aminopyridinium and three tetrathiafulvalenium cations. Another difference is encountered in the interlayer hydrogen bonding network. TTF^{+} cations do not participate in hydrogen bonds whereas the polar 4-aminopyridinium cations are engaged in strong interlayer interactions with the terminal oxalates around chromium(III). The

corrugated character of the anionic layers directly originates from those hydrogen bonds. Nevertheless, the most important conclusion is that in the two cases, *i.e.* whatever the cationic counterpart, the construction of layers of bimetallic trinuclear complexes is favoured compared to the one of 2D (6,3) infinite sheets of bimetallic oxalates because the hydrogen bonds around the Mn(II) ions in the anionic layers compete efficiently with the coordination reaction between terminal oxalates and Mn(II) ions. The subtlety of this competition is indeed an open door upon polymorphism of such network.[17a,21c] Here, the hydrogen bonds impede the formation of a 2D magnet. We shall come back to this point in further papers.

Magnetic properties

The *dc* magnetic properties of **1** and **2** under the form of the $\chi_M T$ *versus* T plot, χ_M being the molar magnetic susceptibility per trinuclear unit, are shown in Fig. 3. At room temperature, the $\chi_M T$ values of 8.14 and 6.3 $cm^3\ mol^{-1}\ K$ for **1** and **2**, respectively, are close to those expected for the sum of two octahedral Cr^{III} ions ($S_{Cr} = 3/2$) ($\chi_M T = 1.87\ cm^3\ mol^{-1}\ K$ with $g_{Cr} = 2.0$) and either one octahedral high-spin Mn^{II} ion ($S_{Mn} = 5/2$) ($\chi_M T = 4.37\ cm^3\ mol^{-1}\ K$, with $g_{Mn} = 2.0$) for **1** or one octahedral high-spin Co^{II} ion ($S_{Co} = 3/2$) with a partially quenched orbital momentum ($\chi_M T = 2.48\ cm^3\ mol^{-1}\ K$ with $g_{Co} = 2.3$) for **2**. Upon cooling, $\chi_M T$ of **1** increases slowly but continuously to reach a value of $\chi_M T$ of 15.80 $cm^3\ mol^{-1}\ K$ at 2.0 K. This value is very close to that expected for a $S = 11/2$ ground state resulting from the intramolecular ferromagnetic coupling between a high-spin Mn^{II} ion ($S = 5/2$) and two Cr^{III} ions ($S = 3/2$) within the $Cr^{III}_2Mn^{II}$ linear triad [$\chi_M T = (N\beta^2 g^2/3k)S(S + 1) = 17.8\ cm^3\ mol^{-1}\ K$ with $g = 2.0$]. For **2**, $\chi_M T$ increases continuously to reach a maximum of 12.2 $cm^3\ mol^{-1}\ K$ at 2.3 K, and then it slightly decreases down to 12.0 $cm^3\ mol^{-1}\ K$ at 2.0 K (inset of Fig. 3). The maximum value of $\chi_M T$ is slightly below than that expected for a $S = 9/2$ ground state resulting from the intramolecular ferromagnetic interaction between the three spin quartets of the

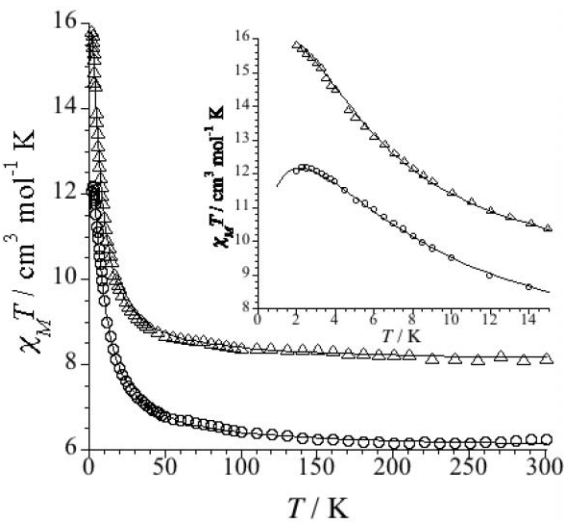

Fig. 3 Temperature dependence of $\chi_M T$ of **1** (△) and **2** (○) (under an applied magnetic field of 1 T ($T \geq 50$ K) and 250 G ($T < 50$ K). The inset shows the maximum of $\chi_M T$ of **2** (○). The solid lines are the best-fit curves (see text).

Table 3 Best-fit magnetic parameters for **1** and **2**

Complex	J^a/cm^{-1}	zj^b/cm^{-1}	$\lvert D_{Co}{}^c \rvert$/cm^{-1}	$g_{Co}{}^d$	$g_{Mn}{}^d$	$g_{Cr}{}^d$	$R^e(\times 10^5)$
1	+1.2	−0.015	0.0	—	1.99	1.99	2.4
2 (fit 1)	+2.6	−0.013	0.0	2.21	—	1.99	5.2
2 (fit 2)	+2.7	0.0	3.7	2.21	—	1.99	6.1

[a] Intramolecular magnetic exchange coupling. [b] Intermolecular magnetic exchange coupling. [c] Axial magnetic anisotropy parameter. [d] Landé factors. [e] Agreement factor $R = \sum[(\chi_M T)_{exp} - (\chi_M T)_{calcd}]^2/\sum[(\chi_M T)_{exp}]^2$.

two terminal Cr^{III} ($S_{Cr} = 3/2$) ions and the central high-spin Co^{II} ($S_{Co} = 3/2$) ion [$\chi_M T = (N\beta^2 g^2/3k)S(S + 1) = 12.4\ cm^3\ mol^{-1}\ K$ with $g = 2.0$]. The decrease of $\chi_M T$ at low temperature is likely due to zero-field splitting (ZFS) effects and/or weak intermolecular antiferromagnetic interactions. The M *versus* H plots for **1** and **2** at 2.0 K, M being the molar magnetization per trinuclear unit, are shown in Fig. S2 (ESI†). The magnetization values of 10.7 and 7.1 $N\beta$ at 5.0 T for **1** and **2** respectively, are consistent with those predicted for a $S = 11/2$ state (**1**) and for a ferromagnetic coupling between a high-spin Co^{II} ion ($S_{eff} = 1/2$ and $g \approx 4.2$)[42] and two Cr^{III} ions ($S = 3/2$, $g = 2.0$) (**2**).

The analysis of the magnetic susceptibility data of compound **1**, was carried out by full-matrix diagonalization[31] of the isotropic spin Hamiltonian for a trinuclear model that takes into account weak intermolecular interactions within the mean field approximation (Table 3) [eqn (1) with $\mathbf{S}_M = \mathbf{S}_{Mn} = 5/2$ and $\mathbf{S}_{Cr1} = \mathbf{S}_{Cr2} = 3/2$]:

$$\mathbf{H} = -J(\mathbf{S_M}\cdot\mathbf{S_{Cr1}} + \mathbf{S_M}\cdot\mathbf{S_{Cr2}}) + zj\langle\mathbf{S_z}\rangle\mathbf{S_z} + g_{Mn}\mathbf{S_M}B + g_{Cr}(\mathbf{S_{Cr1}} + \mathbf{S_{Cr2}})B \quad (1)$$

where J and zj are the intra- and inter-molecular magnetic coupling parameters respectively, and g_{Mn} and g_{Cr} are the Landé factors of the Mn^{II} and Cr^{III} ions.

The least-squares fit of the experimental data are given in Table 3. The Weiss factor $\theta = zjS(S + 1)/3k = -0.16$ K. The fitted curve closely follows the experimental data in the whole temperature range (Fig. 3). The magnetic intermolecular interactions should be related to the hydrogen bonds between trinuclear species in the *ac* plane.

In order to analyse the magnetic susceptibility data of **2**, a first attempt was carried out in a similar manner to **1** using the Hamiltonian (1) with $S_M = S_{Co1} = S_{Cr1} = S_{Cr2} = 3/2$] and $g_M = g_{Co}$. The least-squares fit of the experimental data are given in Table 3. The Weiss factor $\theta = -0.14$ K. The theoretical curve matches very well the experimental one (Fig. 3).

In a second attempt, we considered the magnetic anisotropy of the Co^{II} ions and assumed that the octahedral distortion yields a singlet orbital ground state. The magnetic susceptibility data of **2** was then analysed by full-matrix diagonalization[41] of the spin Hamiltonian (2) for a trinuclear model that takes into account the local axial ZFS of the Co^{II} ion [eqn (2) with $S_{Co} = S_{Cr1} = S_{Cr2} = 3/2$]. The local anisotropy of the six-coordinated Cr(III) is expected to be negligible.

$$\mathbf{H} = -J(\mathbf{S_{Co}}\cdot\mathbf{S_{Cr1}} + \mathbf{S_{Co}}\cdot\mathbf{S_{Cr2}}) + D_{Co}\mathbf{S_{Coz}}^2 + g_{Co}\mathbf{S_{Co}}B + g_{Cr}(\mathbf{S_{Cr1}} + \mathbf{S_{Cr2}})B \quad (2)$$

where the parameters are the same as above and D_{Co} is the axial magnetic anisotropy parameter of the Co^{II} ion. The least-squares fit of the experimental data are given in Table 3. The theoretical

curve closely follows the experimental data for **2**, but the quality of the fit is not improved when compared to that obtained considering intermolecular antiferromagnetic interactions.

The fits results for the magnetic data of **1** and **2** are gathered in Table 3. The magnetic exchange interaction in both compounds is ferromagnetic. This could be expected from the orthogonality of the magnetic orbitals (see discussion below). The weak ferromagnetic intramolecular coupling between the central high-spin Mn^{II} and Co^{II} ion (for **1** and **2**, respectively) and the terminal Cr^{III} ions is similar to that observed in other related oxalato-bridged Cr(III)–Mn(II) and Cr(III)–Co(II) complexes.[21] The lower value of J obtained for **1** when compared to **2** can be explained by the competition between the σ- and π-orbital pathways across the oxalato bridge [ferromagnetic contribution: $(t_{2g})^3(Cr)$–$(e_g)^n(M)$ and antiferromagnetic contribution: $(t_{2g})^3(Cr)$–$(t_{2g})^m(M)$ where n and m are the number of unpaired electrons, $n = 2$ and $m = 3$ for **1** ($M^{II} = Mn^{II}$) and $n = 2$ and $m = 1$ for **2** ($M^{II} = Co^{II}$)]. The antiferromagnetic contribution is smaller than the ferromagnetic contribution in both cases but slightly higher in complex **1**.

Although both complexes possess a large spin ground state ($S = 11/2$ for **1** and $S = 9/2$ for **2**) no out-of-phase signals were observed in the *ac* susceptibility measurements, indicating that a significant negative zero-field splitting ($D_S < 0$) is lacking. This is not surprising for **1**, built from isotropic Cr(III) and high-spin Mn(II) ions. On the contrary, high-spin six-coordinated Co(II) complexes can present a large anisotropy. The parameters extracted from the fit of the experimental magnetic susceptibility for **2** by using a spin-only Hamiltonian [eqn (1)] are relevant only if an important quenching of the first-order orbital angular momentum is involved. On the contrary, by assuming a singlet orbital ground state for Co(II) and neglecting the intermolecular magnetic interactions, we obtained an absolute value for the local zero-field splitting (ZFS) of Co(II), $|D_{Co}| = 3.70$ cm^{-1} which is an upper limit. The corresponding ZFS for the $S = 9/2$ ground state of **2** is related to the local anisotropies as $D_{S=9/2} = (2D_{Cr} + D_{Co})/12$.[43] One obtains $D_{S=9/2} = D_{Co}/12 \approx 0.3$ cm^{-1} by neglecting D_{Cr} leading to an upper limit for the energy barrier $E^{\#} = S^2 D_{S=9/2} \approx 6.3$ cm^{-1}. This small energy barrier could cause a single molecule magnet behaviour below 2 K. $|D_{Co}| = 3.70$ cm^{-1} is an upper limit since we neglected in the fit the intermolecular magnetic interactions that are present in **2**, as observed in **1**. We expect therefore, from experimental data analysis, that D_{Co} should be negligible.

Calculations

We performed electronic structure calculations based on density functional theory for compounds **1** and **2**.

The calculated J values (see Computational details section) for **1** and **2** are –0.05 and +3.4 cm^{-1} using $[MCr_2(ox)_6(H_2O)_2]^{4-}$ models. The calculated value for the $Co^{II}Cr^{III}_2$ complex is in nice agreement with the experimental one (+2.7 cm^{-1}) while the value for $Mn^{II}Cr^{III}_2$ complex indicates a very weak interaction but does not reproduce the ferromagnetic experimental value (+1.16 cm^{-1}). We repeated the calculations increasing the quality of the basis set using a quadruple-ζ and adding the cations around the molecule in order to avoid the negative charge of the model. However, in both cases the J values remain very similar to that initially obtained. The stronger ferromagnetic coupling found for $Co^{II}Cr^{III}_2$ complex, compared to $Mn^{II}Cr^{III}_2$, due to the presence of less antiferromagnetic t_{2g}–t_{2g} contributions is clearly reproduced in the calculations. The predominance of the orthogonality due to the different nature of the magnetic orbitals can be also illustrated in the representation of the spin density (Fig. 4).[44] For the Cr^{III} cations, due to the presence of the unpaired electrons in the t_{2g} orbitals, that are basically non-bonding, the spin polarization mechanism is predominant and the sign of the spin density is negative in the coordinated atoms to the Cr^{III} cations. However, for the Mn^{II} and Co^{II} the presence of unpaired electrons in e_g antibonding orbitals with larger participation of the ligands gives birth to a delocalization mechanism. Thus, the coordinated ligands have the same sign of spin density. It is worth mentioning, that the atoms coordinated to the Cr^{III} cations have two different lobes, one negative corresponding to spin polarization of the σ orbitals, while the white lobe is due to the delocalization on the π system of the ligand.

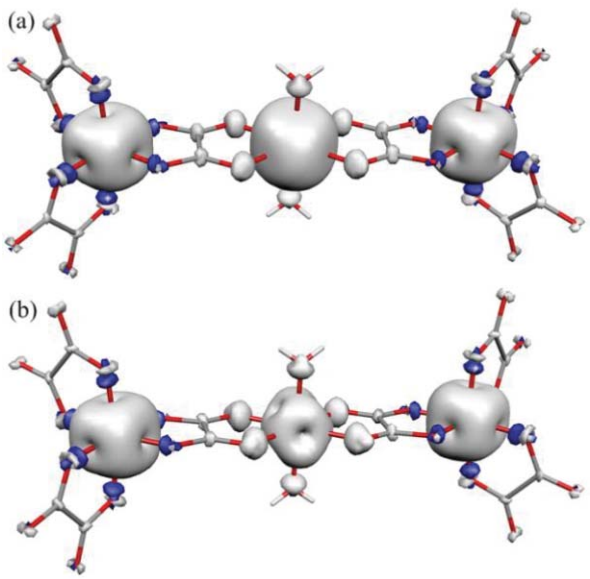

Fig. 4 Calculated spin density corresponding to the high-spin state for the $Mn^{II}Cr^{III}_2$ complex (a) and the $Co^{II}Cr^{III}_2$ complex (b). The isodensity surface corresponds to a value of 0.003 e$^-$/bohr^3 in both cases (positive and negative values are represented as white and blue surfaces, respectively).

We performed the calculation of the zero-field splitting parameter D (see Computational details section) for the $Co^{II}Cr^{III}_2$ complex **2** using a $[CoCr_2(ox)_6(H_2O)_2]^{4-}$ model. The employed approach provides a semiquantitative estimation of such value, and the obtained D value is +0.48 cm^{-1}. This value is due to the spin–orbit contribution because the spin–spin term is negligible (+0.001 cm^{-1}). The calculation of the spin–orbit term using a hybrid functional is done solving the coupled-perturbed SCF equations.[24] From the solution, it is possible to perform a decomposition of the contributions to the D value in the spin-conserving excitations (α–α and β–β) and spin flip terms (α–β and β–α). The analysis of such spin channel contributions indicates that the β–β channel is the predominant term with +0.49 cm^{-1}, the other three contributions being negative and rather small. This value is close but slightly higher, to the upper limit obtained from the fit of the magnetic susceptibility of **2** [$D_{S=9/2} = D_{Co}/12 \approx 0.3$ cm^{-1} (with $D_{Co} = 3.7$ cm^{-1}), see fit 2 in Table 3]. The positive D value

explains the lack of single-molecule magnet behaviour of this system.[19c] It could be expected from the compressed octahedral surrounding of the cobalt.

Conclusions

This contribution illustrates the versatility of the $[Cr(ox)_3]^{3-}$ building block: two trinuclear $[MCr_2]$ [M = Mn(II), Co(II)] species have been synthesized from the mononuclear tris(oxalato)chromate(III) complex acting as a bis-bidentate metalloligand towards fully solvated metal(II) ions. The moderate ferromagnetic coupling between the Cr(III) and the high-spin Mn(II) and Co(II) ions across the oxalate bridges leads to large spin ground states. Nevertheless, the positive sign of the anisotropy of the Co(II) ion in **2** prevents the occurrence of a single molecule magnet (SMM) behaviour as once observed in another oxalate-bridged system.[45]

As previously stated in oxalato-based compounds, through the modulation of the intermolecular interactions, the choice of the cation can influence both the dimensionality and the physicochemical properties of the final compound. Current efforts are devoted to synthesize new compounds using related polar precursors to get non centrosymmetric space groups and valuable dielectric properties.[46]

Acknowledgements

This work was supported by the Centre National de la Recherche Scientifique (CNRS, France), the Ministère de l'Enseignement Supérieur et de la Recherche (MESR, France), the Agence National de la Recherche (ANR, France; project ANR-08-JCJC-0113-01), the Ministerio de Educación y Ciencia (MEC, Spain) (Projects CTQ2007-61690, CSD2007-00010, MAT2007-60660, CTQ2008-06670-C02-01 and CSD2006-00015), Generalitat de Catalunya (2009SGR-1459) and the Magmanet Network of Excellence (Contract 515767-2). E. P. acknowledges the MEC for a postdoctoral grant. The authors thankfully acknowledge the computer resources of *Centre of Supercomputació de Catalunya*.

Notes and references

1 S. Lenninger, B. Olenyuk and J. Stang, *Chem. Rev.*, 2000, **100**, 853.
2 E. Pardo, R. Ruiz-García, J. Cano, X. Ottenwaelder, R. Lescouëzec, Y. Journaux, F. Lloret and M. Julve, *Dalton Trans.*, 2008, 2780.
3 K. L. Scott, K. Wieghardt and A. G. Sykes, *Inorg. Chem.*, 1973, **12**, 655.
4 F. Le Floch, J. Sala Pala and J. Guerchais, *Bull. Soc. Chim. Fr.*, 1975, **1–2**, 120.
5 F. Berezovsky, A. A. Hajem, S. Triki, J. Sala Pala and P. Molinie, *Inorg. Chim. Acta*, 1999, **284**, 8.
6 (*a*) M. Julve, M. Verdaguer, M. F. Charlot and O. Kahn, *Inorg. Chim. Acta*, 1984, **82**, 5; (*b*) M. Julve, M. Verdaguer, A. Gleizes, M. Philoche-Levisalles and O. Kahn, *Inorg. Chem.*, 1984, **23**, 3808.
7 (*a*) F. Pointillart, C. Train, M. Gruselle, F. Villain, H. W. Schmalle, D. Talbot, P. Gredin, S. Decurtins and M. Verdaguer, *Chem. Mater.*, 2004, **16**, 832; (*b*) F. Pointillart, C. Train, F. Villain, C. Cartier dit Moulin, P. Gredin, L.-M. Chamoreau, M. Gruselle, G. Aullon, S. Alvarez and M. Verdaguer, *J. Am. Chem. Soc.*, 2007, **129**, 1327; (*c*) M. Verdaguer, M. Julve, A. Michalowicz and O. Kahn, *Inorg. Chem.*, 1983, **22**, 2624.
8 (*a*) O. Kahn, *Struct. Bonding (Berlin)*, 1987, **68**, 89; (*b*) O. Kahn, *Adv. Inorg. Chem.*, 1995, **43**, 179; (*c*) G. Aromi, S. M. J. Aubin, M. A. Bolcar, G. Christou, H. J. Eppley, K. Folting, D. N. Hendrickson, J. C. Huffman, R. C. Squire, H. L. Tsai, S. Wang and M. W. Wemple, *Polyhedron*, 1998, **17**, 3005; (*d*) D. Gatteschi, A. Caneschi, R. Sessoli and A. Cornia, *Chem. Soc. Rev.*, 1996, **25**, 101.
9 M. Andruh, R. Melanson, C. V. Stager and F. D. Rochon, *Inorg. Chim. Acta*, 1996, **251**, 309.
10 M. C. Muñoz, M. Julve, F. Lloret, J. Faus and M. Andruh, *J. Chem. Soc., Dalton Trans.*, 1998, 3125.
11 F. D. Rochon and G. Massarweh, *Can. J. Chem.*, 1999, **77**, 2059.
12 G. Marinescu, M. Andruh, R. Lescouëzec, M. C. Muñoz, J. Cano, F. Lloret and M. Julve, *New J. Chem.*, 2000, **24**, 527.
13 R. Lescouëzec, G. Marinescu, M. C. Muñoz, D. Luneau, M. Andruh, F. Lloret, J. Faus, M. Julve, J. A. Mata, R. Llusar and J. Cano, *New J. Chem.*, 2001, **25**, 1224.
14 V. Russell, D. Craig, M. Scudder and I. Dance, *CrystEngComm*, 2001, **24**, 1.
15 E. Coronado, M. C. Giménez, C. J. Gómez-García and F. M. Romero, *Polyhedron*, 2003, **22**, 3115.
16 (*a*) H. Tamaki, Z. J. Zhong, N. Matsumoto, S. Kida, M. Koikawa, N. Achiwa, Y. Hashimoto and H. Okawa, *J. Am. Chem. Soc.*, 1992, **114**, 6974; (*b*) S. Decurtins, H. W. Schmalle, P. Schneuwly, J. Ensling and P. Gütlich, *J. Am. Chem. Soc.*, 1994, **116**, 9521; (*c*) M. Gruselle, B. Malézieux, S. Bénard, C. Train, C. Guyard-Duhayon, P. Gredin, K. Tonsuaadu and R. Clément, *Tetrahedron: Asymmetry*, 2004, **15**, 3103; (*d*) M. Clemente-Leon, E. Coronado, J. C. Dias, A. Soriano-Portillo and R. D. Willett, *Inorg. Chem.*, 2008, **47**, 6458; (*e*) Z. Duan, Y. Zhang, B. Zhang and F. L. Pratt, *Inorg. Chem.*, 2009, **48**, 2140.
17 (*a*) E. Coronado, J. R. Galan-Mascaros, C. J. Gomez-Garcia and V. Laukhin, *Nature*, 2000, **408**, 447; (*b*) S. Bénard, P. Yu, J. P. Audière, E. Rivière, R. Clément, J. Guilhem, L. Tchertanov and K. Nakatani, *J. Am. Chem. Soc.*, 2000, **122**, 9444; (*c*) C. Train, R. Gheorghe, V. Krstic, L. M. Chamoreau, N. S. Ovanesyan, L. J. A. Rikken, M. Gruselle and M. Verdaguer, *Nat. Mater.*, 2008, **7**, 729; (*d*) C. Train, T. Nuida, R. Gheorghe, M. Gruselle and S. -I. Ohkoshi, *J. Am. Chem. Soc.*, 2009, **131**, 16838.
18 (*a*) J. K. McCusker, E. A. Schmitt and D. N. Hendrickson, in *Magnetic Molecular Materials*, ed. D. Gatteschi, O. Kahn, J. S. Miller and F. Palacio, Kluwer, Dordrecht, The Netherlands, 1991, 198, 297; (*b*) E. K. Brechin, *Chem. Commun.*, 2005, 5141; (*c*) L. F. Jones, D. M. Low, M. Helliwell, J. Raftery, D. Collison, G. Aromi, J. Cano, T. Mallah, W. Wernsdorfer, E. K. Brechin and E. J. L. Mcinnes, *Polyhedron*, 2006, **25**, 325; (*d*) V. Marvaud, J. M. Herrera, T. Barilero, F. Tuyèras, R. Garde, A. Scuiller, C. Decroix, M. Cantuel and C. Desplanches, *Monatsh. Chem.*, 2003, **134**, 149; (*e*) L. M. C. Beltran and J. R. Long, *Acc. Chem. Res.*, 2005, **38**, 325.
19 (*a*) R. E. P. Winpenny, *Adv. Inorg. Chem.*, 2001, **52**, 1; (*b*) D. Gatteschi and R. Sessoli, *Angew. Chem., Int. Ed.*, 2003, **42**, 268; (*c*) D. Gatteschi, R. Sessoli and J. Villain, *Molecular Nanomagnets*, Oxford University Press, 2006.
20 D. Gatteschi and L. Sorace, *J. Solid State Chem.*, 2001, **159**, 253.
21 (*a*) F. D. Rochon, R. Melanson and M. Andruh, *Inorg. Chem.*, 1996, **35**, 6086; (*b*) E. Coronado, J. R. Galán-Mascarós, C. Giménez-Saiz, C. J. Gómez-García, C. Ruiz-Pérez and S. Triki, *Adv. Mater.*, 1996, **8**, 737–740; (*c*) E. Coronado, J. R. Galán-Mascarós, C. Giménez-Saiz, C. J. Gómez-García and C. Ruiz-Pérez, *Eur. J. Inorg. Chem.*, 2003, 2290; (*d*) N. Stanica, C. V. Stager, M. Cimpoesu and M. Andruh,, *Polyhedron*, 1998, **17**, 1787; (*e*) J. Vallejo, I. Castro, L. Cañadillas-Delgado, C. Ruiz-Pérez, J. Ferrando-Soria, R. Ruiz-García, J. Cano, F. Lloret and M. Julve, *Dalton Trans.*, 2010, **39**, 2350.
22 J. C. Bailar and E. M. Jones, *Inorg. Synth.*, 1939, **1**, 37.
23 (*a*) R. W. W. Hooft, *COLLECT*, Nonius BV, Delft, The Netherlands, 1999; (*b*) A. J. M. Duisenberg, L. M. J. Kroon-Batenburg and A. M. M. Schreurs, *J. Appl. Crystallogr.*, 2003, **36**, 220 (*EVALCCD*).
24 *SADABS*, version 2.03, Bruker AXS Inc., Madison, WI, 2000.
25 G. M. Sheldrick, *SHELX97, Programs for Crystal Structure Analysis (Release 97-2)*, Institüt für Anorganische Chemie der Universität, Göttingen, Germany, 1998.
26 L. J. Farrugia, *J. Appl. Crystallogr.*, 1999, **32**, 837(*WINGX*).
27 (*a*) M. Nardelli, *J. Appl. Crystallogr.*, 1995, **28**, 659; (*b*) D. Palmer, *CrystalMaker*, Cambridge University Technical Services, Cambridge, UK, 1996.
28 (*a*) E. Ruiz, P. Alemany, S. Alvarez and J. Cano, *J. Am. Chem. Soc.*, 1997, **119**, 1297; (*b*) E. Ruiz, J. Cano and S. Alvarez, *Chem.–Eur. J.*, 2005, **11**, 4767; (*c*) E. Ruiz, T. Cauchy, J. Cano, R. Costa, J. Tercero and S. Alvarez, *J. Am. Chem. Soc.*, 2008, **130**, 7420.
29 (*a*) E. Ruiz, *Struct. Bond.*, 2004, **113**, 71; (*b*) E. Ruiz, S. Alvarez, J. Cano and V. Polo, *J. Chem. Phys.*, 2005, **123**, 164110; (*c*) E. Ruiz, J. Cano, S. Alvarez and P. Alemany, *J. Comput. Chem.*, 1999, **20**, 1391; (*d*) E. Ruiz,

A. Rodríguez-Fortea, J. Cano, S. Alvarez and P. Alemany, *J. Comput. Chem.*, 2003, **24**, 982.
30 E. Ruiz, A. Rodríguez-Fortea, J. Tercero, T. Cauchy and C. Massobrio, *J. Chem. Phys.*, 2005, **123**, 074102.
31 A. D. Becke, *J. Chem. Phys*, 1993, **98**.
32 A. Schaefer, C. Huber and R. Ahlrichs, *J. Chem. Phys.*, 1994, **100**, 5829.
33 F. Weigend, F. Furche and R. Ahlrichs, *J. Chem. Phys.*, 2003, **119**, 12753.
34 M. J. Frisch, G. W. Trucks, H. B. Schlegel, G. E. Scuseria, M. A. Robb, J. R. Cheeseman, G. Scalmani, V. Barone, B. Mennucci, G. A. Petersson, H. Nakatsuji, M. Caricato, X. Li, H. P. Hratchian, A. F. Izmaylov, J. Bloino, G. Zheng, J. L. Sonnenberg, M. Hada, M. Ehara, K. Toyota, R. Fukuda, J. Hasegawa, M. Ishida, T. Nakajima, Y. Honda, O. Kitao, H. Nakai, T. Vreven, J. A. Montgomery, Jr., J. E. Peralta, F. Ogliaro, M. Bearpark, J. J. Heyd, E. Brothers, K. N. Kudin, V. N. Staroverov, R. Kobayashi, J. Normand, K. Raghavachari, A. Rendell, J. C. Burant, S. S. Iyengar, J. Tomasi, M. Cossi, N. Rega, J. M. Millam, M. Klene, J. E. Knox, J. B. Cross, V. Bakken, C. Adamo, J. Jaramillo, R. Gomperts, R. E. Stratmann, O. Yazyev, A. J. Austin, R. Cammi, C. Pomelli, J. Ochterski, R. L. Martin, K. Morokuma, V. G. Zakrzewski, G. A. Voth, P. Salvador, J. J. Dannenberg, S. Dapprich, A. D. Daniels, O. Farkas, J. B. Foresman, J. V. Ortiz, J. Cioslowski and D. J. Fox, *GAUSSIAN 09 (Revision A.1)*, Gaussian, Inc., Wallingford, CT, 2009.
35 *Jaguar 7.0*, Schrödinger, LLC, New York, 2007.
36 G. Vacek, J. K. Perry and J.-M. Langlois, *Chem. Phys. Lett.*, 1999, **310**, 189.
37 *Orca 2.7.0*, F. Neese, Bonn, 2005.
38 (*a*) F. Neese, *J. Am. Chem. Soc.*, 2006, **128**, 10213; (*b*) F. Neese, *J. Chem. Phys.*, 2007, **127**, 164112.
39 S. Zein and F. Neese, *J. Phys. Chem. A*, 2008, **112**, 7976.
40 E. H. Merrachi, B. F. Mentzen and F. Chassagneux, *Rev. Chim. Minér.*, 1986, **23**, 329.
41 J. Cano, *VPMAG package*, University of Valencia, Valencia, Spain, 2003.
42 F. Lloret, M. Julve, J. Cano, R. Ruiz-García and E. Pardo, *Inorg. Chim. Acta*, 2008, **361**, 3432.
43 A. Bencini and D. Gatteschi, *Electron paramagnetic resonance of exchange coupled systems*, Berlin, New York, Springer-Verlag, 1990.
44 (*a*) J. Cano, E. Ruiz, S. Alvarez and M. Verdaguer, *Comments Inorg. Chem.*, 1998, **20**, 27; (*b*) E. Ruiz, J. Cirera and S. Alvarez, *Coord. Chem. Rev.*, 2005, **249**, 2649.
45 J. Martínez-Lillo, D. Armentano, G. De Munno, W. Wernsdorfer, M. Julve, F. Lloret and J. Faus, *J. Am. Chem. Soc.*, 2006, **128**, 14218.
46 H. Cui, Z. Wang, K. Takahashi, Y. Okano, H. Kobayashi and A. Kobayashi, *J. Am. Chem. Soc.*, 2006, **128**, 15074.

